The air quality in narrow two-dimensional urban canyons with pitched and flat roof buildings

Simone Ferrari*, Maria Grazia Badas, Michela Garau, Alessandro Seoni and Giorgio Querzoli

DICAAR - Dipartimento di Ingegneria Civile, Ambientale e Architettura, Università degli Studi di Cagliari,
via Marengo 2, 09123 Cagliari, Italy
Email: ferraris@unica.it
Email: mgbadas@unica.it
Email: mi.garau@unica.it
Email: aseoni@unica.it
Email: querzoli@unica.it
*Corresponding author

Abstract: The aim of this paper is the study of the air quality in narrow urban canyons (ratio of the distance between two buildings to the building height equal to one). This have been done investigating two key points. The first one is the investigation of the modifications that the roof shape induces in the flow and turbulence, through the comparison of velocity fields, turbulence characteristics and air exchanges between the urban canyon and the outer flow in arrays of buildings with flat and pitched roof. The second one is the assessment of the capability of a RANS model to correctly simulate the flow, through the comparison with laboratory water-channel simulations. Among the analysed quantities the vertical air-exchange rate ACH measures the rate of air removal from a street canyon. Results show that the pitched roof strongly modifies the flow and increases the turbulence and the air exchange between the canyon and the external flow, highlighting how the choice of the roof shape can be meaningful for building design, planning strategies and regulatory purposes.

Keywords: narrow urban canyon, air quality, natural ventilation, pitched roof, RANS simulation, laboratory simulation.

Reference to this paper should be made as follows: Author. (xxxx) 'Title', *Int. J. xxxxxxxxxx xxxxxxxxxx*,

Biographical notes:

Simone Ferrari has been an Aggregate Professor in Fluid Mechanics at the University of Cagliari (Italy), since 2011. He received his PhD in Territorial Engineering from the University of Cagliari, in collaboration with the Imperial College London (UK) in 2007. His research interests include turbulence and mixing in civil, environmental, industrial and biological flows.

Maria Grazia Badas has been an Aggregate Professor in Hydraulics II at the University of Cagliari (Italy), since 2006. She received her PhD in Territorial Engineering from the University of Cagliari in 2005. Her research topics include turbulence and mixing in civil, environmental and biological flows.

Author

Michela Garau is a PhD student in Civil Engineering and Architecture. Her main research interests include boundary layer meteorology, numerical modelling of urban canopies and dispersion models.

Alessandro Seoni has been a Graduate Technician in Hydraulics and Hydraulic Structures and Infrastructures since 2007. He has been teaching assistant at the University of Cagliari in Hydrology and Hydraulic Structures since 2008, and in Hydraulics since 2013. He received his PhD in Territorial Engineering in 2014 from the University of Cagliari, Italy. His research interests include turbulence, Hydrology and flow measurements.

Giorgio Querzoli has been a Full Professor in Fluid Mechanics at the University of Cagliari, Italy since 2006. He received his PhD in Environmental Monitoring at the University of Florence, Italy in 1996. He teaches 'Hydraulics' and 'Environmental hydraulics'. His research topics are turbulence and dispersion in biologic and environmental flows, such as atmospheric boundary layer and ocean outfalls.

This paper is a revised and expanded version of a paper entitled The air quality in two-dimensional urban canyons with gable roof buildings: a numerical and laboratory investigation presented at the 17th International conference on Harmonisation within Atmospheric Dispersion Modelling for Regulatory Purposes. Budapest, Hungary, May 9-12, 2016.

The paper is submitted for a special issue with László Bozó and Zita Ferenczi as guest editors.

1 Introduction

Even if the air flow and its turbulence in the urban environment are known to be biased by the geometrical shape of the buildings (see, for example, Raifailidis 1997, Xie et al. 2005, Takano and Moonen 2013), most of the fluid dynamic investigations were typically performed on flat roof buildings (e.g. Sato et al., 2011, Leung et al., 2012, Di Bernardino et al. 2015-b), even in the last years. Moreover, narrow urban canyons, i.e. those with a low aspect ratio W/H (that is $W/H < 1$, where W is the distance between two buildings and H is the height of the buildings, see Fig.1), are the most widespread urban canopies in the old centres of many European cities. Furthermore, in areas with strong rainfalls or snowfalls the buildings tend to have pitched roofs (Kellnerova et al., 2008) and, in some regions, building codes prescribe a minimum slope. Ntinas et al. (2014) and Tominaga et al. (2015) investigated, via both wind tunnel and numerical simulations, the modifications induced in the flow by pitched and/or arched roof, highlighting the influence on the flow of the shape of the roof but in an isolated building. Kellnerova et al. (2012) performed wind tunnel experiments on an array of flat and pitched roof buildings but focusing on the detection of large organized structures via Proper Orthogonal Decomposition (POD). Yassin (2011) and Badas et al. (2017) numerically simulated, via Reynolds Averaged Navier-Stokes (RANS) models, the flow in array of buildings with different roof shapes, but without focusing on velocity high order statistics. Vice-versa, Addepalli and Pardyjak (2013) and Di Bernardino et al. (2015b) measured velocity statistics, respectively, up to the second and third order in their laboratory experiments but in flat roof buildings only.

As a consequence, the main aim of this paper is the study of the air quality in narrow urban canyons with flat and pitched roof, via the characterization of the velocity statistics up to the third order. In order to achieve this goal, we have dealt with two main aspects.
The first one is the investigation and assessment of the effect of pitched roofs on the air flow and turbulence in narrow urban canyons when compared to flat roof ones. In order to do that, we have performed a water-channel laboratory simulation, investigating via Feature Tracking Velocimetry (a non-intrusive image analysis technique) the velocity fields and the turbulence characteristics in urban canyons, formed by identical buildings with flat or symmetrical dual-pitched roofs and a constant flow perpendicular to the canyon axis, and an aspect ratio W/H = 1 (i.e. a condition where, according to Oke 1988, a skimming flow develops in case of flat roof buildings). In order to achieve this target, we have performed a statistical analysis taking into account velocity statistics from the first to the third order, able to better highlight characteristic flow and turbulence features.
The second target of this paper is the assessment of the capability of a Reynolds Averaged Navier-Stokes (RANS) model to correctly simulate the air flow in narrow urban canyons, with both flat and pitched roof buildings. With this target, RANS simulations were performed by means of a model, described hereafter, and their results were compared with the ones from laboratory water-channel simulations. This RANS model, if validated, could allow to perform numerical simulations of urban canyons in a more convenient and rapid way, with respect to both laboratory simulations and more complex numerical approaches. As a matter of fact, as stated by Blocken in his 2015 review on Computational Fluid Dynamics for Urban Physics, the computational cost of RANS models is at least an order of magnitude lower than for LES (Large Eddy Simulation) models, so many researchers and practitioners still use RANS models.

2 Materials and methods

As previously stated, both in laboratory and numerical simulations, we have investigated the flows in urban canyons, formed by identical buildings with flat roofs or symmetrical dual-pitched roofs (45°), a canyon aspect ratio W/H = 1 and a constant flow perpendicular to the canyon axis, which is one of the worst condition for air ventilation and pollution removal from the canyon.

2.1 Laboratory simulations

Laboratory experiments have been performed in a closed-loop water-channel, with glass walls, in the Hydraulic Laboratory of the University of Cagliari - Italy. The channel is 50 cm high, 40 cm wide and 800 cm long, with a honeycomb screen in the first part (to uniform the flow) and a floodgate in the end (to set the desired water depth, flow rate and, consequently, velocity in the test section). The canyon array consists in 20 identical buildings: 2 cm high and wide parallelepipeds (see Fig. 1a) were chosen, in order to have an obstruction factor less than 5% (as required by Barlow et al., 1999 to properly reproduce the full scale phenomena). The symmetrical dual pitched roof buildings were built adding a 45° pitched roof to the parallelepipeds representing the flat roof buildings (Fig.1b and 1c). The test section is located at around 650 cm downstream of the channel inlet, where the neutral boundary layer can be considered fully-developed. Small pebbles, with an equivalent diameter of 0.5 cm were displaced over the channel bottom for 300 cm upstream the canyon array, in order to increase the roughness of the bottom and to

reproduce a logarithmic velocity profile. In order to perform velocity measurements via an image analysis technique (namely Feature Tracking Velocimetry, FTV, see below), the fluid was seeded with non-buoyant particles (pine pollen), the test section was lighted by a green laser sheet and images were recorded by a high-speed camera at the resolution of 2240 x 1760 px and 200 Hz (Fig. 2). The Reynolds number Re, based on the canyon height, is about 5,000, largely higher than the minimum value of 3,400 suggested, among the others, by Hoydysh (1974) for the flow to be independent on the Reynolds number. Similar values have been more recently proposed by Yee et al., 2006 (Re ≈ 4,000) and by Pournazeri et al., 2012 (Re = 4,600), and employed in water tunnel experiments on urban canyons by Di Bernardino et al., 2015a and 2015b (Re in the range 3,545÷4,480).
As stated, Feature Tracking Velocimetry (FTV, Besalduch et al 2013 and 2014) has been employed to measure velocity and turbulence fields. The advantages of image analysis techniques, when compared to traditional probes, are substantial (see Ferrari 2017 for a review): they are non-intrusive, quasi-continuous in space (as each pixel on an image can be considered as a virtual probe) and allow to perform a wide range of measurements, e.g. the concentration fields of a substance in the environment (e.g. Strang and Fernando 2004, Ferrari and Querzoli 2010), the position of the free surface of a wave train over a breakwater (Ferrari and Querzoli 2015, Ferrari et al. 2016) or the velocity (e.g. Badas and Querzoli 2011, Di Bernardino et al 2015-a) and acceleration of a fluid flow (Ferrari and Rossi 2008). FTV has proved to be less sensitive to the appearance and disappearance of particles, and to high velocity gradients than classical Particle Image Velocimetry (PIV). More details on FTV can be found in Besalduch et al. (2013 and 2014).

2.2 Numerical simulations

Numerical simulations have been performed by means of the open source CFD library OpenFOAM 2.3.1 (Weller et al. 1998). A Reynolds Averaged Navier-Stokes model (RANS) with two equation k-ε closure (Launder and Spalding, 1974) was set up; simpleFoam (Patankar and Spalding, 1972), a steady state solver for incompressible turbulent flows (which adopts the SIMPLE algorithm) and second order schemes for spatial discretization were employed. A uniform, indefinite succession of buildings was simulated by imposing periodic boundary conditions in the streamwise direction. Re, based on the canyon height, is about 43,000, largely higher than the minimum value of 15,000 suggested by Snyder (1981) for the flow to be independent on Re.
The simulation domain is two-dimensional, three canyons long in the streamwise direction, and 15 H high, minimizing unphysical accelerations due to blockage effects. The numerical set up and the mesh is chosen in order to fulfill the condition reported for flow simulation around buildings (domain height, grid resolution, cell stretching ratio, grid sensitivity analysis) in the best practice guidelines of Franke et al. (2011) and by Blocken (2015). A grid sensitivity analysis was performed for the flat roof case: four grids were tested (large, medium, fine and very fine). According to the guidelines, the coarsest mesh has 10 cells per building side, the minimum number suggested, whilst the other ones are obtained doubling the cell number in each direction (total number of cells spans from 860 for the large grid to 55040 for the very fine one). Simulations here presented refer to the fine grid (hence 40 cells per building side), since a further increase in cell number was proven not to influence the results. Moreover, different turbulent parametrizations were tested, without obtaining an improvement in reproducing laboratory data. For an in-depth description of the numerical set-up the reader is referred to Badas et al (2017)

Cyclic boundary conditions were imposed at the inlet and outlet for all the variables, except for pressure, whose gradient is adjusted to obtain the required mean velocity. The upper boundary of the computational domain was considered a symmetry plane. At ground and building surfaces no-slip conditions were imposed for velocity, while Neumann zero gradient conditions were imposed for pressure and turbulent quantities (kinetic energy k, energy dissipation rate and turbulent viscosity). The non-dimensional vertical momentum flux $<u_i'u_j'>$ was computed as follows:

$$< u_i' u_j' >= -\nu_t \left(\frac{\partial < u_i >}{\partial x_j} + \frac{\partial < u_j >}{\partial x_i} \right) + \frac{2}{3} \delta_{ij} k \quad (1)$$

where ν_t is the turbulent viscosity, computed as follows:

$$\nu_t = C_\mu \frac{k^2}{\varepsilon} \quad (2)$$

and

$$C_\mu = 0.09 \quad (3)$$

u' is the fluctuation of the velocity around its mean value, while <·> denotes the average value.

OpenFOAM has been already extensively and successfully used to perform wind RANS simulation in urban environment (e.g. Hertwig et al. 2012); moreover, Takano and Moonen (2013) proved that a similar OpenFOAM configuration was able to properly reproduce a two-dimensional periodic array of flat roof buildings. Here we want to investigate the capability of the code above described to properly reproduce the fluid dynamics of the flow over an array of pitched roof buildings as well.

3 Results

In all the figures showing velocities or turbulence characteristics fields, the flow moves from the left to the right. The mean velocity fields and profiles (first order statistics), both from experimental and numerical simulations, will be shown first, to then illustrate the second order statistics (vertical momentum flux and variance of the velocity), the skewness factors (third order statistics) and close with the vertical air-exchange rate (integral parameter). The step-like shape of the pitched roof in Figure 8, 14, 17, 18, 21 and 22 is due to the grid of the data elaboration close to the roof in experimental data.

3.1 Mean velocity fields and profiles

Fig.3 shows the non-dimensional mean velocity field u/U (i.e. the mean velocity magnitude u non-dimensionalised by the mean free stream velocity U, measured at Z/H = 7) for flat roof, obtained from numerical simulations, with some streamlines in white. Fig.4 shows the same case from the laboratory simulations. The stable single vortex (with the centre with the horizontal coordinate X/H very close to 0 and the vertical

one Z/X slightly above 0.5), typical of the skimming flow regime illustrated, for instance, in Oke (1988) and measured in their wind tunnel experiment by Kellnerova et al. (2012) and in their water tunnel experiments by Di Bernardino et al. (2015a), is well reproduced, as well as the two small counter-rotating vortices at the bottom corners of the cavity. The velocity magnitude and, in general, the streamlines appear to be correctly reproduced from the numerical simulations.

In Fig.5 the vertical profiles of the horizontal component of the non-dimensional velocity U_X/U are drawn, from numerical (continuous red lines) and laboratory (dashed blue lines) simulations; the profiles are measured in the middle of the canyon (X/H = 0, left side) and above the middle of a building roof (X/H = 1, right side). Fig.6 shows the same measures but for the vertical component U_Z/U. The U_X/U profiles are correctly reproduced, both for positive and negative velocities, from the numerical code, even if with an overestimation of the velocity magnitude (always lower than the 20%). The U_Z/U profiles show that the numerical model tends to smooth the deviation in the streamlines due to the cavity, with an underestimation of the velocity magnitude outside the cavity. Inside the canyon, the numerical model seems not able to catch the negative and positive values of the vertical velocity, even if we have to notice that these are very small.

Similar considerations apply to Fig.7 and Fig.8 (u/U fields for pitched roof from numerical and laboratory simulations respectively), as the numerical code is able to reproduce the modifications induced in the flow features by the pitched roof, i.e. the upwards displacement of the main vortex centre and its deformation (in agreement with the findings of Kellnerova et al., 2012), even if the effect of the pitched roofs in reducing the velocity outside the canyon (or, in other words, the vertical size of the main vortex) is slightly underestimated by the numerical simulations. As a matter of fact, in the case of flat roof the outer flow is almost unperturbed (with a steep increase of the velocity with Z and the free stream velocity U almost reached at Z/H = 3), whilst the case of pitched roof determines a perturbation that propagates significantly above the roof, with wavy streamlines also above the ridge of the roof and a zone of reduced velocity that extends upwards that is larger than in the flat roof case. It is quite interesting the appearance of a hyperbolic stagnation point, in the middle of the upstream side of the downstream building's roof, separating the zone were the air flow enters into the canyon from the one where it skims above the building. Moreover, the roof pitch causes an increase in the size of the counter-rotating vortex at the downstream bottom corners of the cavity. We can consequently state that the pitched roof biases the flow, strongly modifying its topology.

Fig.9 and Fig.10 (vertical profiles of the horizontal component of the velocity U_X/U and of the vertical one U_Z/U, respectively, for the case of pitched roof) show a remarkable capability of the numerical code in simulating the velocity horizontal component, whilst some differences can be found, as in the case of flat roof, for the vertical component. In particular, the increase in the value of the vertical component of the velocity is relevant if compared with the flat roof case (Fig.6), as this implies a faster displacement of the air and, consequently, an easier exchange of air between the canyon and the outer flow.

3.2 Vertical momentum flux

Fig.11 shows the field of the non-dimensional vertical momentum flux $\langle u'w' \rangle / U^2$ from numerical simulations, in the case of flat roof; here u' is the fluctuation of the horizontal velocity around its mean value, w' is the fluctuation of the vertical velocity. In Fig.12, the same quantity from laboratory simulations is shown. The numerical code is able to correctly simulate the vertical momentum flux both outside the canyon, where values are

negative (e.g. Di Bernardino et al. 2015a), and inside the canyon, where it catches the transitions from negative to positive values. In particular, the tongue-like structure propagating from the upper corner of the downstream building is properly reproduced. Anyway, the comparison between Fig. 11 and 12 shows that the RANS code tends to overestimate the vertical momentum flux values, both in the canyon and in the free flow region outside the cavity.

The maps of non-dimensional vertical flux for the pitched roof case are depicted in Fig.13 (numerical simulations) and 14 (laboratory simulations). In this case, as in the one of flat roof, the RANS code correctly simulates the trend of the field but with an overestimation of both the negative and positive values and without catching the peaks due to the roof edges at X/H = -1 and X/H = 1.

When comparing the vertical momentum flux in the case of flat (Fig.12) and pitched roof (Fig.14), the modifications induced by this last configuration are clear: positive values increase their magnitude, in particular close to the upstream side of the downstream building's roof, where the vertical momentum flux has a peak, highlighting where there is the largest penetration of air from the outer flow.

We can consequently state that the RANS numerical code applied here is able to properly reproduce laboratory investigations, even if with some weaknesses in the velocity second order statistics: these last are intimately connected to the parameterization of turbulence that is at the base of all the RANS models.

3.3 Variance of the velocity

In Fig.15 the field of the non-dimensional variance of the horizontal component of the velocity $\langle u'^2 \rangle / U^2$ is shown, while Fig.16 illustrates the non-dimensional variance of the vertical component of the velocity $\langle w'^2 \rangle / U^2$, both for the flat roof case and the laboratory simulations. Velocity variance is a measure of the intensity of turbulent fluctuations, i.e. of the stirring induced in the air by the flow: this is a relevant parameter in a statistical analysis of turbulent flows and, in particular, in air quality investigations, because the higher the stirring, the stronger the mixing between fresh air from the outer flow and air from the canyon will be, with consequently better quality for the air inside the canyon. It is known (see, for instance, Di Bernardino et al. 2015a) that $\langle u'^2 \rangle / U^2$ has lower values inside the cavity than outside (Fig.15), while $\langle w'^2 \rangle / U^2$ has large values on the upper part of the downstream side of the cavity, with a tongue-like shape highlighting the penetration of turbulence from the outer flow inside the canyon (Fig.16).

On Fig.17 and Fig. 18, $\langle u'^2 \rangle / U^2$ and $\langle w'^2 \rangle / U^2$ for the pitched roof case are reported (laboratory simulations). It is evident how the pitched roof induces higher value of variance of the velocity components (i.e. turbulent fluctuations) in the outer flow. Moreover, the penetration of the variance of the vertical velocity component from the outer flow into the cavity is larger (see, in Fig.18, the magnitude and size of the tongue-like structure on the downstream side if the canyon) and, differently from the flat case, is evident for the variance of the horizontal velocity component as well (see, in Fig.17, the tongue-like structure on the roof of the downstream building). Moreover, also above the cavity the $\langle w'^2 \rangle / U^2$ values in the pitched roof case are around twice the corresponding ones in the flat roof case. As a consequence, the penetration of turbulent fluctuations inside the canyon and, consequently, the mixing of air from the outer flow with the air inside the cavity is clearly enhanced by the pitched roof.

3.4 Skewness factors

Fig.19 shows the field of the non-dimensional skewness factor of the horizontal component of the velocity $<u'^3>/<u'^2>^{3/2}$, while Fig.20 reports the field of the non-dimensional skewness factor of the vertical component of the velocity $<w'^3>/<w'^2>^{3/2}$, both for the flat roof case. The same quantities are shown in Fig.21 and Fig.22 but for the pitched roof case. Skewness gives a measure of the asymmetrical distribution of values around the mean: if a distribution has positive skewness values, then the probability density function has a longer right tail (strongest positive fluctuations), whilst if a distribution has negative skewness, then the probability density function has a longer left tail. Moreover, the study of the skewness factors is meaningful as they are included in the Lagrangian stochastic models of turbulent diffusion in atmosphere (see, for instance, Rodean 1996). The black lines, with zero values, highlight where there is a transition from positive to negative values. Values inside the canyon are generally larger than the ones in the outer flow, highlighting a more uniform distribution of turbulent fluctuations in the outer flow. In agreement with Di Bernardino et al., 2015a, the skewness factor of the horizontal component of the velocity inside the canyon is negative almost everywhere, except, as stated above, in the dark red tongue at the top of the canyon. This dark red tongue in Fig.19 seems to show that the turbulence generated by the shear stress of the flow against the upstream building's roof has a strongly asymmetrical distribution of fluctuations that creates a barrier to the penetration of the air from the outer flow into the cavity. The skewness factor of the vertical velocity has positive values on the left vertical side of the canyon and negative ones on the right side. When comparing the flat roof case with the pitched roof one (Fig.21), it is clear that this barrier is less pronounced, thus fostering the air exchange. Moreover, if in the flat roof case the zones of positive and negative skewness have almost the same area, for both the horizontal and vertical components, in the case of pitched roof the area of negative skewness occupies almost all the cavity.

3.5 Vertical air-exchange rate

As previously stated, the air quality and the comfort in an urban canyon depend essentially on the air exchanges between the canyon and the overlying boundary layer. We have so investigated the vertical air-exchange rate, ACH (Ho and Liu, 2014, Ho et al., 2015), which is an integral parameter measuring the rate of air removal from a street canyon, depending on the mean and turbulent flow (<ACH> and ACH ', respectively):

$$ACH = < ACH > + ACH' = \int_b < w_+ > dx + \frac{1}{2}\int_b \sqrt{< w'^2 >}\, dx \qquad (4)$$

where $< w_+ >$ is the mean upward velocity, at the roof ridge height, b is the horizontal line at Z/H = 1, from X/H = -0.5 to X/H = 0.5, connecting two consecutive buildings (hence, in the present work b = W, both in case of flat roof and pitched roof) and $< w'^2 >$ is estimated, under the assumption of isotropic turbulence, as:

$$\overline{w'^2} = -2\nu_t\left(\frac{\partial \bar{w}}{\partial z}\right) + \frac{2}{3}k \qquad (5)$$

The advantage of using an integral parameter such as ACH lies in its capability to describe in a single number the effect on the air quality of the different building configurations: higher ACH values imply a higher exchange of air between the outer flow

and the canyon and can imply, as a consequence, a better air quality for the people inside the canyon. Table 1 shows the ACH (non-dimensionalised by U·b) and its components for flat and pitched roof.
The values of ACH from numerical simulations are very similar to the ones measured in the laboratory. Moreover, the turbulent component of ACH is predominant (57% in the case of pitched roof, between 86% and 95% in the case of flat roof), suggesting that the city ventilation is dominated by the ACH turbulent component (that is, the air is mainly driven by atmospheric turbulence). This is in agreement with what was found in the numerical simulations on flat roof canyons by Ng and Liu (2014), who found values of ACH' larger than 60% of the ACH, and in the wind tunnel measurements by Ho and Liu (2014), who found values of at least 80%. More relevant is the fact that the ACH values for pitched roof are always much higher than the flat roof ones (1.92 times larger according to experimental simulations), showing that pitched roofs tend to enhance the natural ventilation inside the canyon.

4 Conclusions

We have investigated, both via numerical and laboratory simulations, the effect of symmetrical dual-pitched roofs, on the air quality in narrow urban canyons with aspect ratio equal to one.
The RANS numerical code applied here has shown to be able to properly reproduce laboratory investigations, particularly regarding the flow shape and its first order statistics, but with some weaknesses in the second order statistics, intimately connected to the parameterization of turbulence at the base of all the RANS models.
Both numerical and laboratory simulations show that the flow topology and turbulence are strongly affected by the shape of the roof, with the pitched roof that is abler than the flat roof to modify the outer flow, to increase turbulence and to enhance the vertical momentum flux. In particular, the pitched roof increases the vertical velocity variance, the penetration of turbulent fluctuations inside the canyon and, consequently, the mixing of air from the outer flow with the air inside the cavity. This is due to the reduction of the barrier (to the vertical flow) generated by the strong asymmetrical distribution of the horizontal velocity fluctuations, highlighted by the skewness fields.
An integral parameter, the air exchange rate ACH, has been used to summarize the results: also in this case, both numerical and laboratory investigations have highlighted the meaningful role of the pitched roof in increasing the air exchange rate between the urban canyon and the outer flow, thus promoting pollutant and heat dispersion.
As a consequence, we can state that in the simplified configuration adopted, consisting of periodic and identical 2D buildings subject to perpendicular and constant wind, the employment of pitched roofs is a way to increase the air quality in narrow urban canyons. The present results could have an immediate practical impact on the building design and on planning strategies, as the roof shape can be a useful tool to enhance natural ventilation and pollutant or heat dispersion, i.e. the air quality in urban areas.

5 References

Addepalli B. and Pardyjak E.R., 2013: Investigation of the flow structure in step-up street canyons—mean flow and turbulence statistics. *Boundary-Layer Meteorol*, **148**, 133-155.

Badas M.G. and Querzoli G., 2011: Spatial structures and scaling in the Convective Boundary Layer. *Exp Fluids*, **50**(4), 1093-1107.

Badas M.G., Ferrari S., Garau M. and Querzoli G, 2017: On the effect of gable roof on natural ventilation in two-dimensional urban canyons. *J Wind Eng Ind Aerodyn*, **162**, 24-34.

Barlow J.B., Rae W.H. and Pope A., 1999: Low-speed wind tunnel testing. Third Edition. Wiley.

Besalduch L.A., Badas M.G., Ferrari S. and Querzoli G., 2013: Experimental Studies for the characterization of the mixing processes in negative buoyant jets. *Eur Phys J WoC*, **45**, 01012.

Besalduch L.A., Badas M.G., Ferrari S. and Querzoli G., 2014: On the near field behavior of inclined negatively buoyant jets. *Eur Phys J WoC*, **67**, 02007.

Blocken B., 2015: Computational fluid dynamics for urban physics: importance, scales, possibilities, limitations and ten tips tricks toward accurate and reliable simulations. *Build Envir*, **91**, 1-27.

Di Bernardino A., Monti P., Leuzzi G. and Querzoli G., 2015-a: Water-channel study of flow and turbulence past a 2D array of obstacles. *Bound-Layer Meteorol*, **155**(1), 73–85.

Di Bernardino, A., Monti, P., Leuzzi, G. and Querzoli, G., 2015-b: On the effect of the aspect ratio on flow and turbulence over a two-dimensional street canyon, *Int. J. of Environment and Pollution*, **58**, 27 - 38.

Ferrari S. and Rossi L., 2008: Particle tracking velocimetry and accelerometry (PTVA) measurements applied to quasi-two-dimensional multi-scale flows. *Exp Fluids*, **44**, 873-886.

Ferrari S. and Querzoli G., 2010: Mixing and re-entrainment in a negatively buoyant jet. *J Hydraul Res*, **48**, 632-640.

Ferrari S. and Querzoli G., 2015: Laboratory experiments on the interaction between inclined negatively buoyant jets and regular waves. *Eur Phys J WoC*, **92**, 02018.

Ferrari S., Badas M.G. and Querzoli G., 2016. A non-intrusive and continuous-in-space technique to investigate the wave transformation and breaking over a breakwater. *Eur Phys J WoC*, **114**, 02022.

Ferrari S., 2017: Image analysis techniques for the study of turbulent flows. *Eur Phys J WoC*, **143**, 01001.

Franke J., Hellsten A., Schlunzen K.H. and Carissimo B, 2011: The COST 732 Best Practice Guideline for CFD simulation of flows in the urban environment: a summary. *Int J Environ Pollut*, **44**, 419.

Hertwig D., Efthimiou G.C., Bartzis J.G. and Leitl B.,2012: CFD-RANS model validation of turbulent flow in a semi-idealized urban canopy. *J Wind Eng Ind Aerodyn*, **111**, 61–72.

Hoydysh W.G., Griffths R.A. and Owaga Y.A., 1974: Scale Model Study of the Dispersion of Pollution in Street Canyons, *Proceedings of the 67th Annual Meeting of the Air Pollution Control Assn.*, Denver, Colorado (USA), June 9-13.

Ho Y.K. and Liu C.H. 2014: Experimental study on flow and ventilation behaviours over idealised urban roughness. *Int. J. of Environment and Pollution*, **54**, 110 - 118.

Ho Y.K., Liu C.H. and Wong M.S., 2015: Preliminary study of the parameterisation of street-level ventilation in idealised two-dimensional simulations. *Build Environ*, **89**:345–355.

Huang Y., Hu X. and Zeng N., 2009: Impact of wedge-shaped roofs on airflow and pollutant dispersion inside urban street canyons. *Build Environ.*, **44**, 2335–2347.

Kellnerova R. and Jaiour Z., 2008: The flow instabilities within an urban intersection. *Int. J. of Environment and Pollution*, **47**, 268 - 277.

Kellnerova R., Kukacka L., Jurcakova K., Uruba V. and Janour Z., 2012: PIV measurement of turbulent flow within a street canyon: detection of coherent motion. *J Wind Eng Ind Aerodyn*, **104-106**, 302-313.

Launder B.E. and Spalding D.B., 1974: The numerical computation of turbulent flows. Comput Methods *Appl Mech Eng* **3**, 269–89.

Leung K.K. and Liu Chun-Ho, 2012: Local mass transfer coefficients over idealized two-dimensional urban street canyons information. *Int. J. of Environment and Pollution*, **50**, 75 - 82.

Ng C-T. and Liu C-H, 2014: Numerical simulations of street canyon ventilation and pollutant dispersion. *Int. J. of Environment and Pollution*, **55**, 167 – 173.

Ntinas G.K., Zhang G., Fragos V.P., Bochtis D.D. and Nikita-Martzopoulou C., 2014: Airflow patterns around obstacles with arched and pitched roofs: Wind tunnel measurements and direct simulation. *Eur J Mech B/Fluids*, **43**, 216-229.

Oke TR. 1988: Street design and urban canopy layer climate. *Energy Build*, **11**, 103–113.

Patankar S. and Spalding D., 1972: A calculation procedure for heat, mass and momentum transfer in three-dimensional parabolic flows. *Int J Heat Mass Transf*, **15**, 1787–806.

Pournazeri S., Princevac M. and Venkatram A., 2012: Scaling of building affected plume rise and dispersion in water channels and wind tunnels — Revisit of an old problem. *J Wind Eng Ind Aerodyn*, **103**, 16-30.

Rafailidis S. 1997: Influence of Building Areal Density and Roof Shape on the Wind Characteristics Above a Town. *Bound-Layer Meteorol*, **85**, 255–271.

Rodean H.C., 1996: *Stochastic Lagrangian Models of Turbulent Diffusion*. American Meteorological Society, 1-87.

Sato A., Michioka T. and Takimoto H., 2011: Field experiments of flow and dispersion within a street canyon in outdoor urban scale model. *Int. J. of Environment and Pollution*, **47**, 184 - 192.

Snyder W.H., 1981: Guideline for fluid modeling of atmospheric diffusion. vol. 81. Environmental Sciences Research Laboratory, Office of Research and Development, US EPA, EPA-600/8-81-009.

Strang E.J. and Fernando H.J.S., 2004: Shear-induced mixing and transport from a rectangular cavity, *J Fluid Mech*, **520**, 23-49.

Takano Y. and Moonen P., 2013: On the influence of roof shape on flow and dispersion in an urban street canyon. *J Wind Eng Ind Aerodyn*, **123**, Part A:107–120.

Tominaga Y., Akabayashi S.-I., Kitahara T. and Arinami, Y., 2015: Air flow around isolated gable-roof buildings with different roof pitches: Wind tunnel experiments and CFD simulations. *Build Environ*, **84**, 204-213.

Weller H.G., Tabor G., Jasak H. and Fureby C., 1998: A tensorial approach to computational continuum mechanics using object-oriented techniques. *Comput Phys*, **12**, 620–631.

Xie X, Huang Z, Wang J. 2005: Impact of building configuration on air quality in street canyon. *Atmos Environ*, **39**, 4519–4530.

Yassin MF., 2011: Impact of height and shape of building roof on air quality in urban street canyons. *Atmos Environ*, **45**, 5220–5229.

Yee E., Gailis R.M., Hill A., Hilderman T. and Kiel D., 2006: Comparison of wind-tunnel and water-channel simulations of plume dispersion through a large array of obstacles with a scaled field experiment. *Bound-Layer Meteorol*, **121**, 389–432.

6 Figures

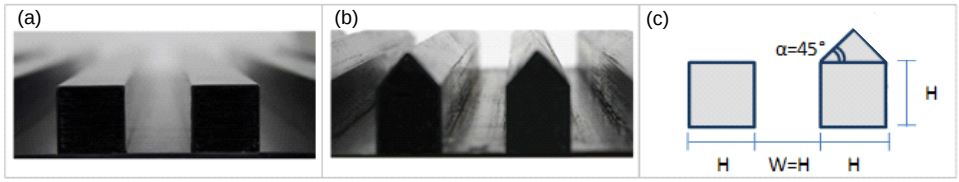

Figure 1. Urban canyon configuration: (a) detail of the array of flat roof buildings for the laboratory simulations; (b) detail of the array of pitched roof buildings for the laboratory simulations; (c) model dimensions for both numerical and laboratory simulations, with H = W = 2 cm.

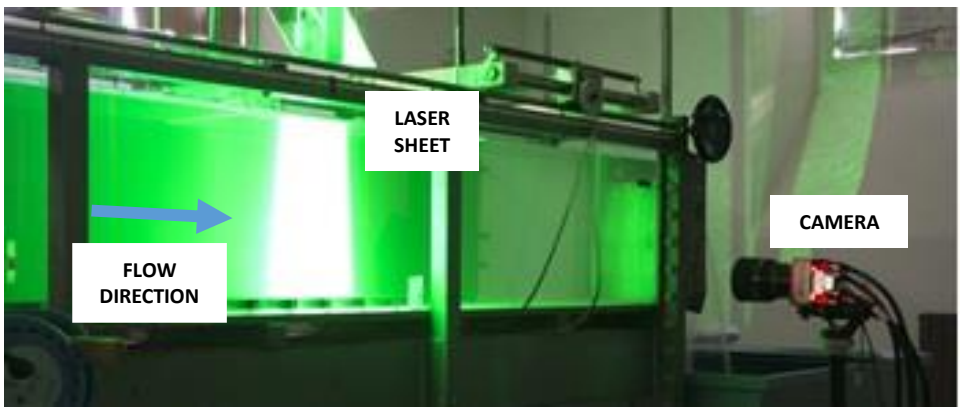

Figure 2. Laboratory set-up.

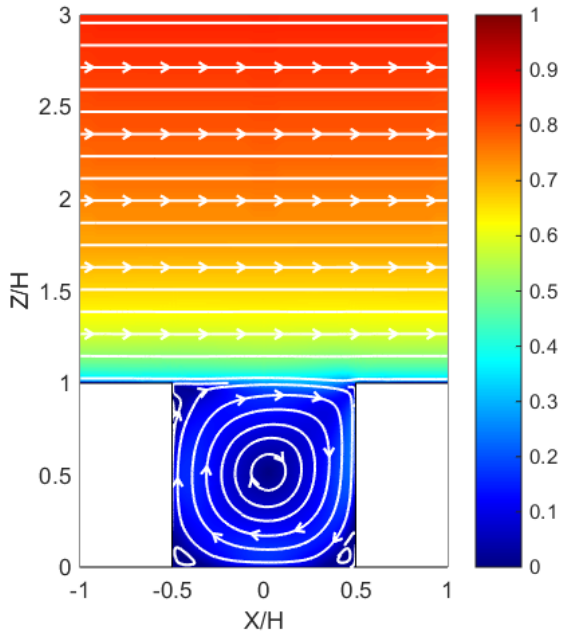

Figure 3. Non-dimensional mean velocity u/U field (color map) with streamlines (white lines) from numerical simulations, for flat roof.

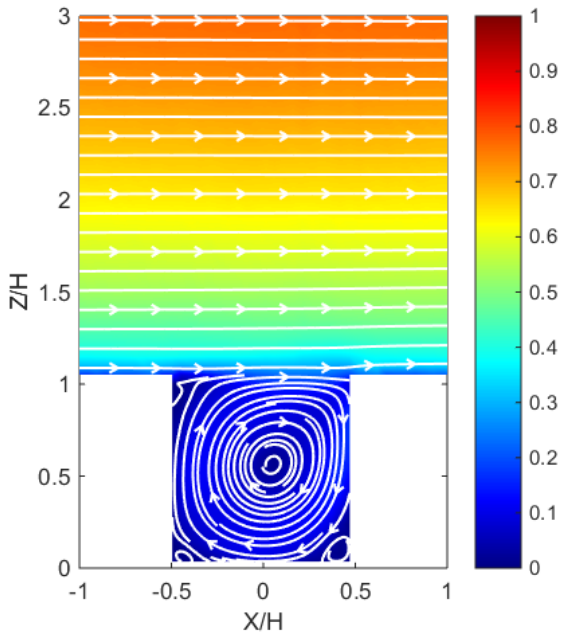

Figure 4. Non-dimensional mean velocity u/U fields (color map) with streamlines (white lines) from laboratory simulations, for flat roof.

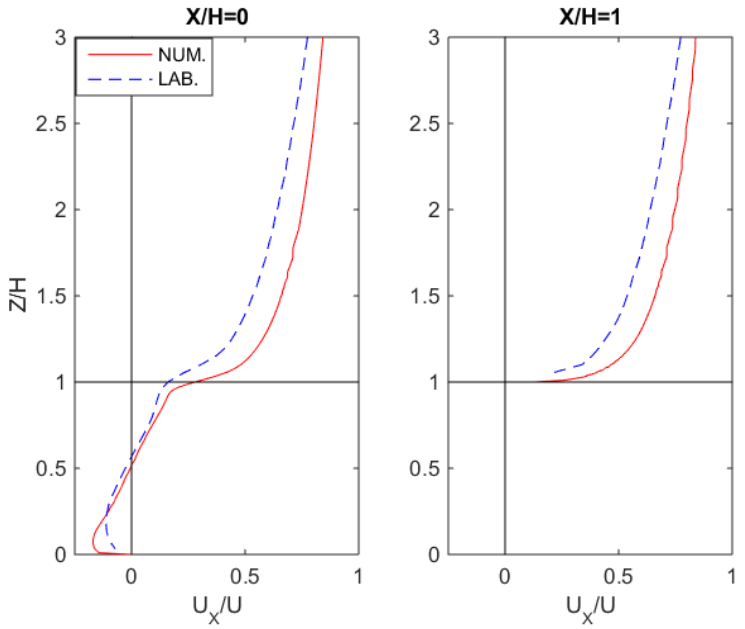

Figure 5. Vertical profiles of the non-dimensional horizontal component of the velocity U_X/U for flat roof; on the left, X/H = 0 (middle of the canyon), on the right, X/H = 1 (middle of the roof); dashed blue line: laboratory simulations, continuous red line: numerical simulations.

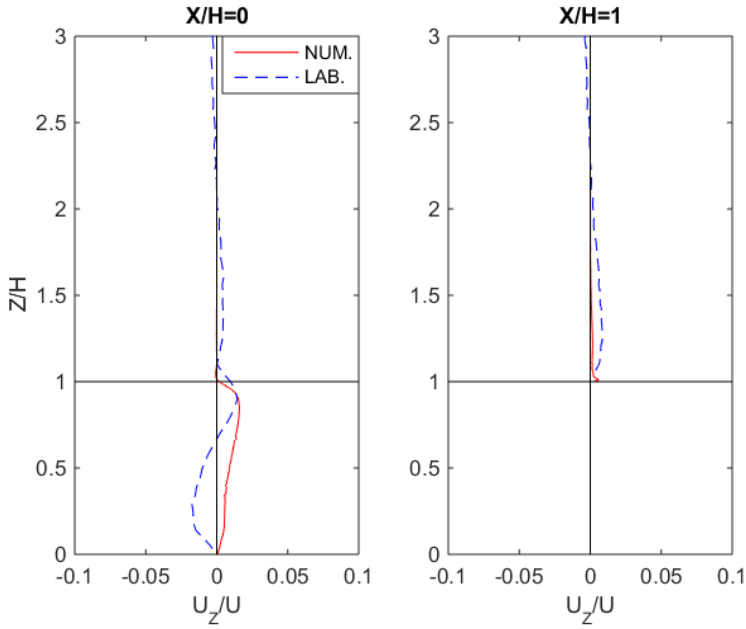

Figure 6. Vertical profiles of the non-dimensional vertical component of the velocity U_Z/U for flat roof; on the left, X/H = 0 (middle of the canyon), on the right, X/H = 1 (middle of the roof); dashed blue line: laboratory simulations, continuous red line: numerical simulations.

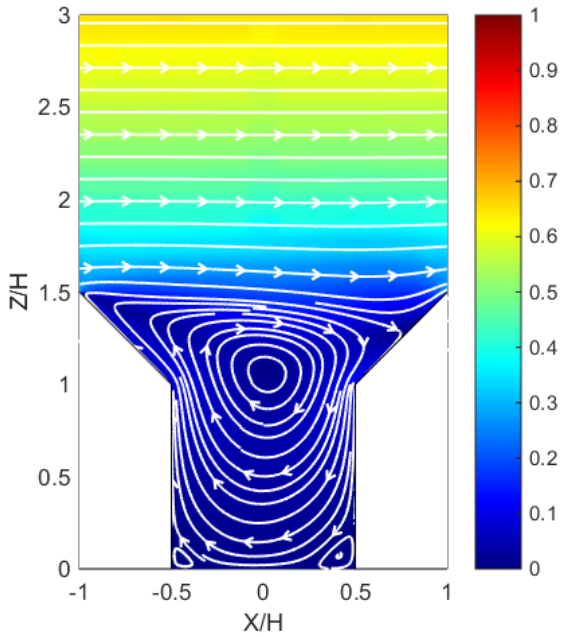

Figure 7. Non-dimensional mean velocity u/U field (color map) with streamlines (white lines) from numerical simulations, for pitched roof.

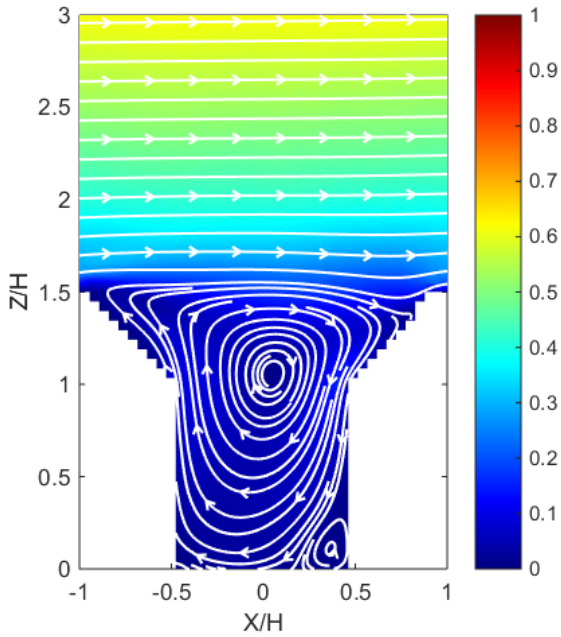

Figure 8. Non-dimensional mean velocity u/U field (color map) with streamlines (white lines) from laboratory simulations, for pitched roof.

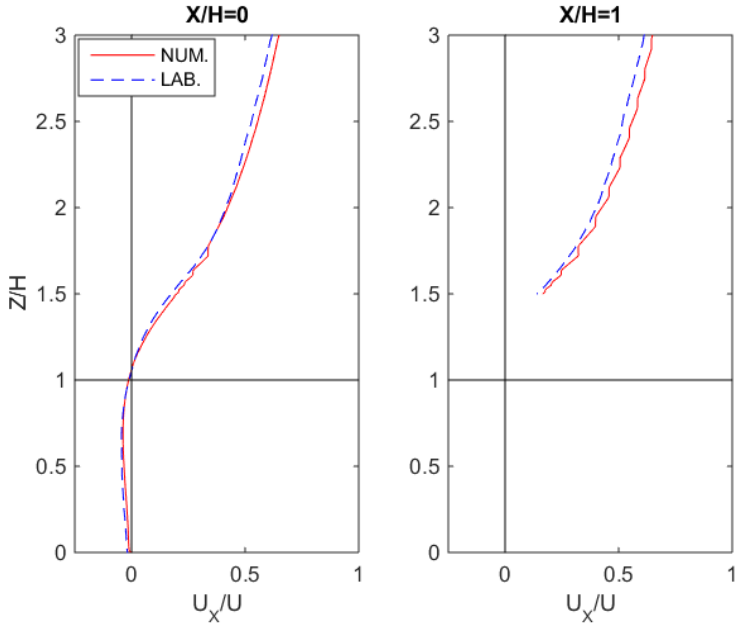

Figure 9. Vertical profiles of the non-dimensional horizontal component of the velocity U_X/U for pitched roof; on the left, X/H = 0 (middle of the canyon), on the right, X/H = 1 (middle of the roof); dashed blue line: laboratory simulations, continuous red line: numerical simulations.

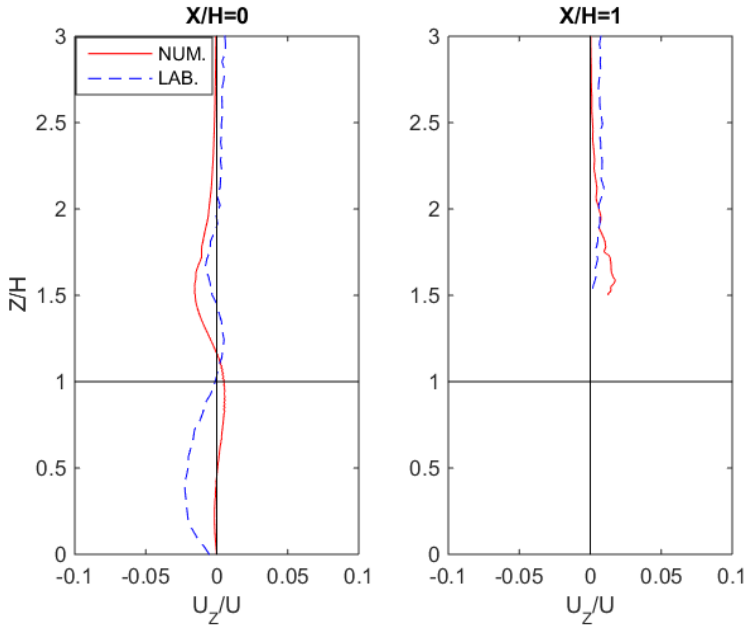

Figure 10. Vertical profiles of the non-dimensional vertical component of the velocity U_Z/U for pitched roof; on the left, X/H = 0 (middle of the canyon), on the right, X/H = 1 (middle of the roof); dashed blue line: laboratory simulations, continuous red line: numerical simulations.

Author

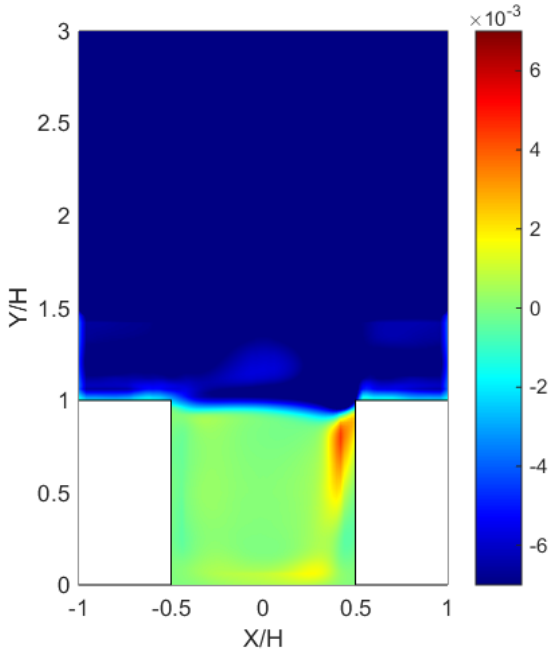

Figure 11. Non-dimensional vertical momentum flux <u'w'>/U² fields (color map) from numerical simulations, for flat roof.

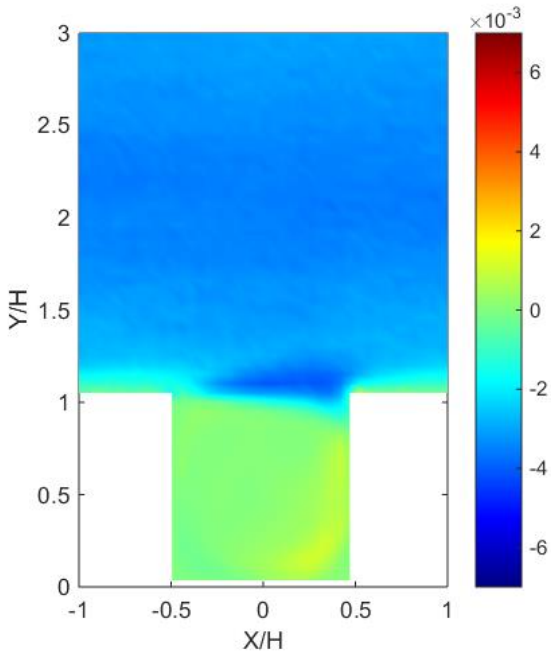

Figure 12. Non-dimensional vertical momentum flux <u'w'>/U² fields (color map) from laboratory simulations, for flat roof.

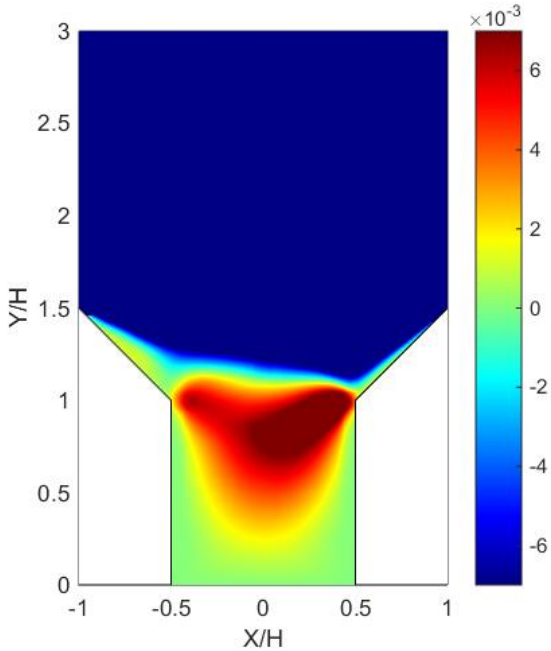

Figure 13. Non-dimensional vertical momentum flux <u'w'>/U^2 fields (color map) from numerical simulations, for pitched roof.

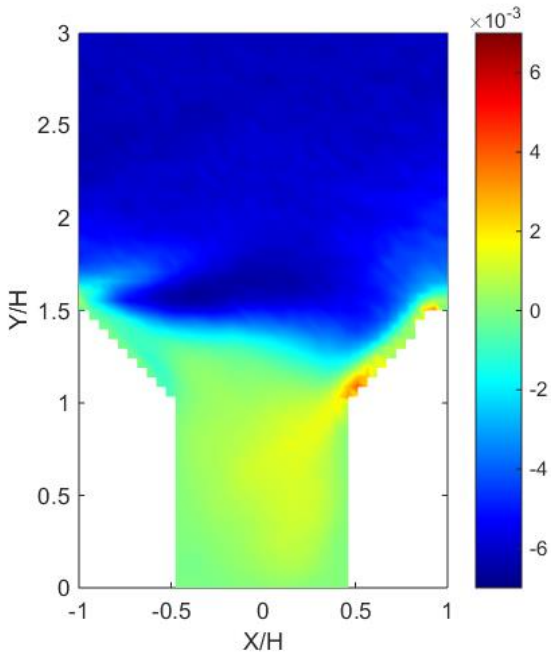

Figure 14. Non-dimensional vertical momentum flux <u'w'>/U^2 fields (color map) from laboratory simulations.

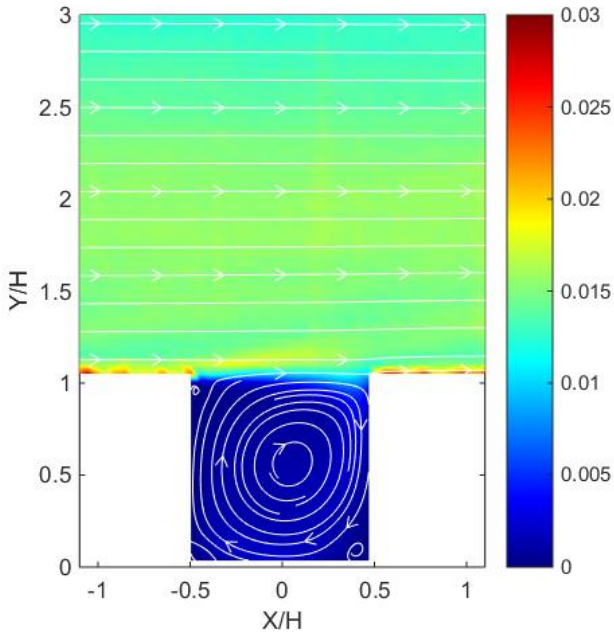

Figure 15. Field of the non-dimensional variance of the horizontal component of the velocity $\langle u'^2 \rangle / U^2$ (color map) with streamlines (white lines) from laboratory simulations, for flat roof.

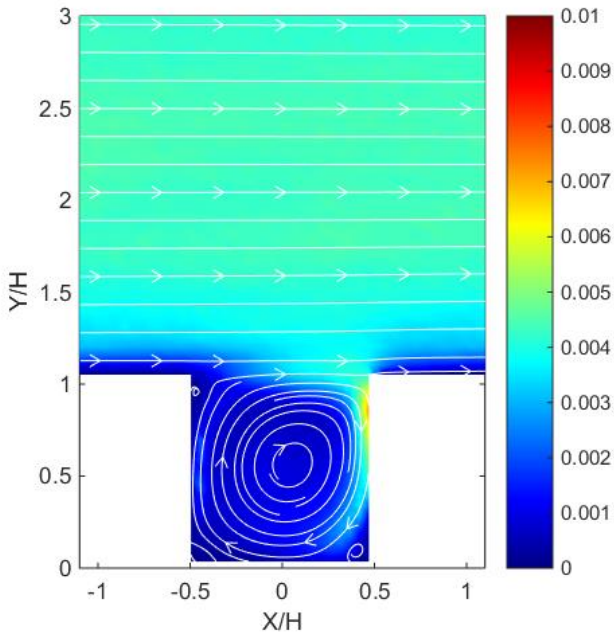

Figure 16. Field of the non-dimensional variance of the vertical component of the velocity $\langle w'^2 \rangle / U^2$ (color map) with streamlines (white lines) from laboratory simulations, for flat roof.

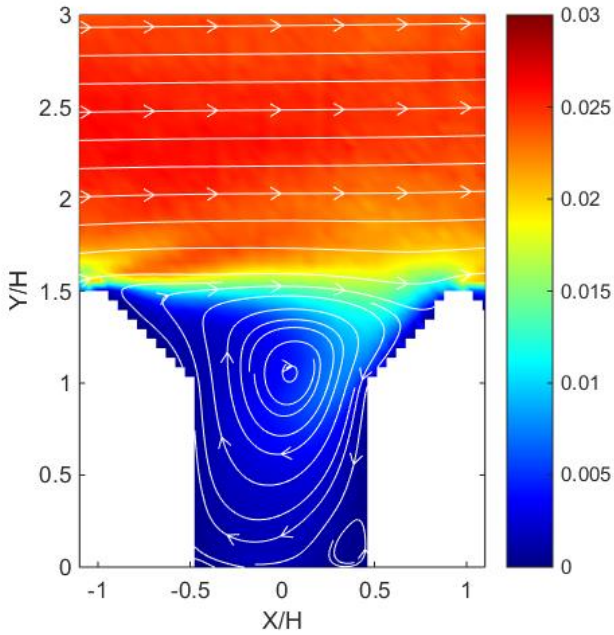

Figure 17. Field of the non-dimensional variance of the horizontal component of the velocity $\langle u'^2 \rangle / U^2$ (color map) with streamlines (white lines) from laboratory simulations, for pitched roof.

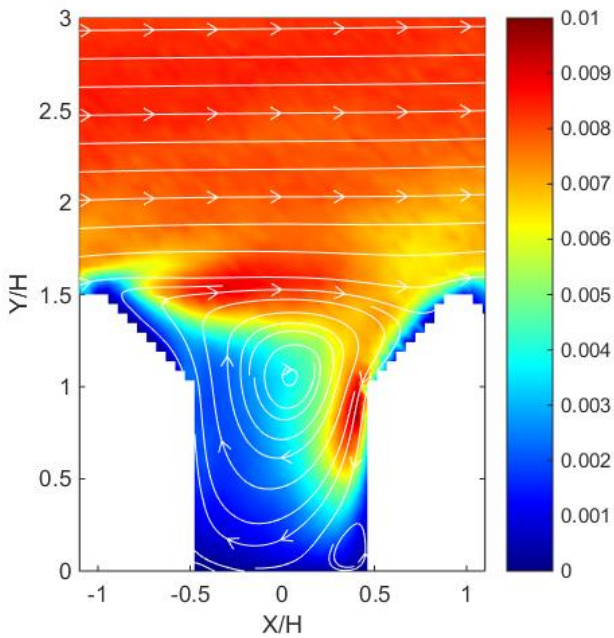

Figure 18. Field of the non-dimensional variance of the vertical component of the velocity $\langle w'^2 \rangle / U^2$ (color map) with streamlines (white lines) from laboratory simulations, for pitched roof.

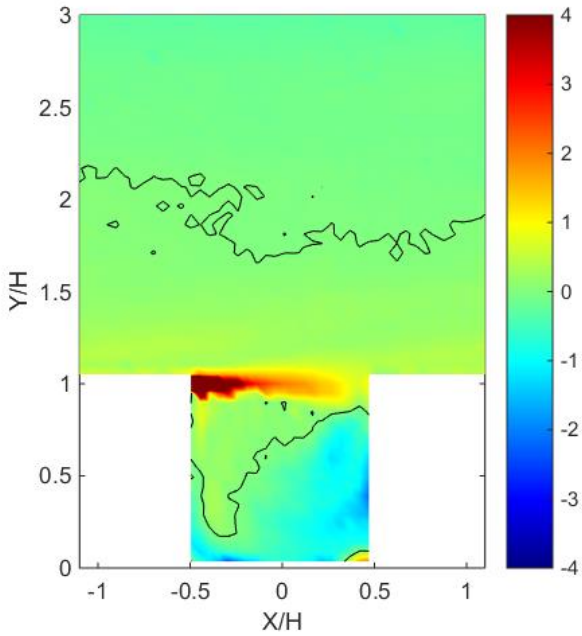

Figure 19. Field of the non-dimensional skewness factor of the horizontal component of the velocity $\langle u'^3 \rangle / \langle u'^2 \rangle^{3/2}$ from laboratory simulations, for flat roof; black lines highlight the zero values.

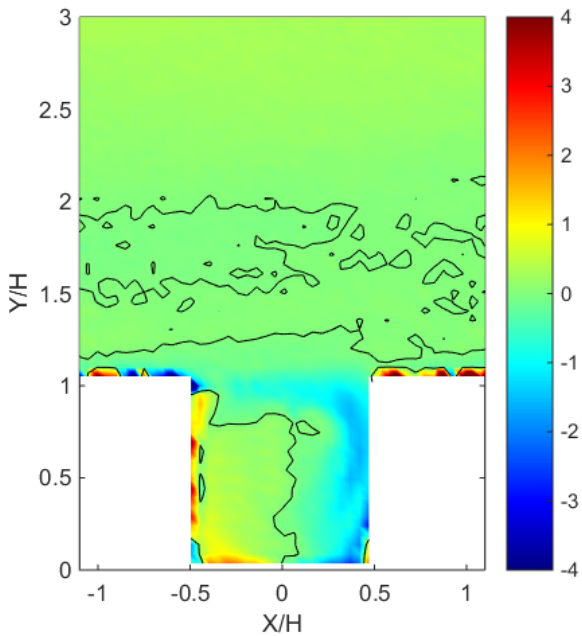

Figure 20. Field of the non-dimensional skewness factor of the vertical component of the velocity $\langle w'^3 \rangle / \langle w'^2 \rangle^{3/2}$ from laboratory simulations, for flat roof; black lines highlight the zero values.

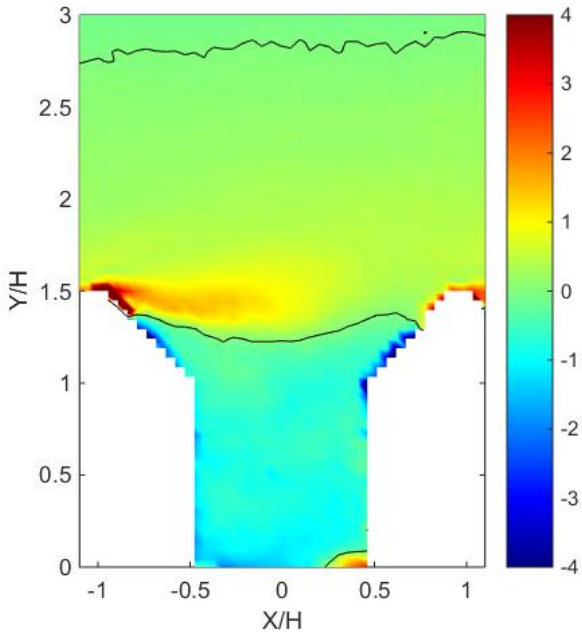

Figure 21. Field of the non-dimensional skewness factor of the horizontal component of the velocity $\langle u'^3 \rangle / \langle u'^2 \rangle^{3/2}$ from laboratory simulations, for pitched roof; black lines highlight the zero values.

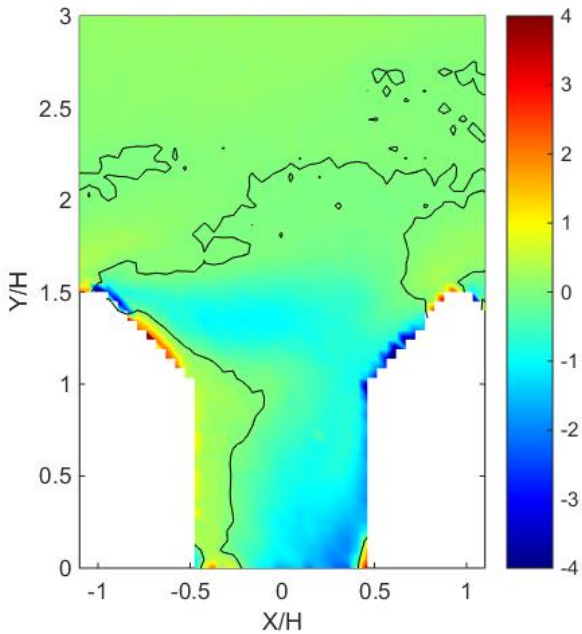

Figure 22. Field of the non-dimensional skewness factor of the vertical component of the velocity $\langle w'^3 \rangle / \langle w'^2 \rangle^{3/2}$ from laboratory simulations, for pitched roof; black lines highlight the zero values.

Author

	LABORATORY		NUMERICAL	
	FLAT	**PITCHED**	**FLAT**	**PITCHED**
ACH	0.0237	0.0454	0.0312	0.0491
<ACH>	0.0009	0.0191	0.0041	0.0212
ACH'	0.0227	0.0259	0.0269	0.0279

Table 1. ACH values from laboratory and numerical simulations.